Check for updates

Wet-chemistry assembly of one-dimensional nanowires: switching characteristics of a known spin-crossover iron(II) complex through Raman spectroscopy†

Zoi G. Lada, [a] Athanassios Chrissanthopoulos, [b] Spyros P. Perlepes,*[ac]
Konstantinos S. Andrikopoulos *[ad] and George A. Voyiatzis*[a]

In this study, a simple, fast, one-pot approach for the isolation of nanowires (NWs) in coordination chemistry is reported. Nanowires (NWs) of spin-crossover (SCO) materials are extremely rare. Here, an innovative and easy synthetic process was developed to prepare NWs of a switchable polymorph of the known complex *trans*-[Fe(NCS)$_2$(abpt)$_2$] using a wet-chemistry approach for the first time; abpt is the bidentate chelating ligand 4-amino-3,5-bis(pyridin-2-yl)-1,2,4-triazole. The remarkable smoothness of the high-spin to low-spin transition, monitored through variable-temperature (300−80 K) Raman microscopy, compared with the sharp transition exhibited by the polycrystalline material, demonstrates the effect of the topological properties on the physical phenomena of the system.

With the discovery of carbon nanotubes, scientists have developed an intense interest in the preparation of other one-dimensional (1D) structures, such as nanorods, nanobelts and nanowires (NWs).[1–3] These structures exhibit better properties from those of bulk materials, because of the large surface-to-volume ratios. NWs have many applications in photonic and electronic, biomedical, and energy conversion and storage devices.[2,4–8] Strategies for the growth of NWs are available.[2,3,9] As concerns magnetic NWs, their preparation by implementation of thin film etching[10,11] and template-assisted electrodeposition routes[12–14] has already been reported. All these multiple step synthetic/preparation methods could be considered time-consuming and thus lack direct technological prospects, while simple one pot methods are still scarce.

Spin-crossover (SCO) complexes[15–20] present molecular bistability due to the fact that the molecules can switch between two electronic states differing in the number of unpaired electrons (high-spin, HS, and low-spin, LS) which is caused due to an external stimuli, *e.g.* temperature, pressure and light irradiation. Several applications have been envisaged or realized, such as data storage as well as display technologies and sensor uses.[21–25] SCO complexes have been reintroduced in the last 15 years or so, based on the entirely new pathways opened by controlling their properties and switching capabilities in the nanoscale.[26–30] As stated in the now seminal review by Bousseksou, Molnar and co-workers,[26] the new era is a consequence of the development of synthetic routes to produce nanosized SCO nanoparticles (NPs) and nanopatterned thin films, as well as of the use of high-resolution experimental techniques and theoretical approaches that enable the study of spatiotemporal phenomena in cooperative SCO systems. The two routes widely used for the preparation of SCO NPs, *i.e.* direct fabrication based on batch-mode synthesis,[31] and the templating approach which uses hard inorganic and organic templates,[31,32] suffer from some disadvantages.[31] Recently the groups of Chastanet and Aymonier reported a unique, template-free continuous process to isolate NPs of a SCO coordination polymer using supercritical CO$_2$ for both quenching the NP growth and drying the powder. This method results in the isolation of well-defined and dried NPs at large scale, while simultaneously reduces the preparation time.[31] Several nanosized (NPs and thin films) SCO systems are described in the above mentioned review[26] together with the corresponding relationships between size-morphology and switching characteristics. However, the authors wrote: *"We are not aware of any reports on one-dimensional (1D) SCO nanomaterials, such as nanowires or nanotubes".* The only to date successful report along this line is the smart synthesis of NWs of a thermal SCO Fe(III) complex by its template assembly in nanoporous anodic aluminum oxide.[32]

a Institute of Chemical Engineering Sciences (ICE-HT), Foundation for Research and Technology-Hellas (FORTH), Platani, P.O. Box 1414, Patras 26504, Greece. E-mail: zoilada@iceht.forth.gr, perlepes@patreas.upatras.gr, kandriko@upatras.gr, gvog@iceht.forth.gr

b Laboratory of Inorganic Chemistry, Department of Chemistry National and Kapodistrian University of Athens Panepistimiopolis, Zografou 15771, Athens, Greece. E-mail: achryssan@chem.uoa.gr

c Department of Chemistry, University of Patras, Panepistimiopolis, Patras 26504, Greece

d Department of Physics, University of Patras, Panepistimiopolis, Patras 26504, Greece

† Electronic supplementary information (ESI) available. See DOI: 10.1039/d1cc05802a
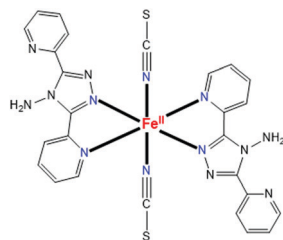
Scheme 1 General schematic structure of the trans-$[Fe^{II}(NCS)_2(abpt)_2]$ molecules that are present in polymorphs **A**, **B**, **C** and **D** of this complex.

Fig. 1 SEM images of the polymorph **A** of trans-$[Fe(NCS)_2(abpt)_2]$ at two different magnifications. The dashed circles indicate the presence of white-greyish grains assigned to polymorph **B** (see text).

Herein we report for the first time the synthesis of nanowires of a known SCO complex through entirely wet chemistry. This extremely easy, convenient and low-cost wet-chemistry synthetic approach represents an advantage for potential future applications. In addition to the synthesis, we describe the full study of its switching characteristics through Raman spectroscopy and DFT calculations. Raman spectroscopy is a powerful technique with which temperature-induced SCO behavior can be followed;[33,34] however, it has been rarely employed in coordination chemistry in the nanoscale.[32,35–39] The known complex used is trans-$[Fe^{II}(NCS)_2(abpt)_2]$ (Scheme 1), where abpt is 4-amino-3,5-bis(pyridin-2-yl)-1,2,4-triazole. This complex is known to exist in four well-characterized polymorphs (**A**, **B**, **C**, **D**).[40–44] **A** has one independent Fe^{II} site in the asymmetric unit,[40,44] whereas **C** and **D** both possess two crystallographically independent Fe^{II} ions.[42,43] The only polymorph that remains in the HS state in the whole 300–2 K range is **B**.[41] Polymorph **A** is a SCO system with a $T_{1/2}$ value of ∼190 K.[40,44] Since **A** contains only one unique Fe^{II} site in the asymmetric unit and exhibits a well-characterized, complete SCO transition triggered by temperature, our studies focus on this polymorph. Another two favorable parameters (which are also valid for some other polymorphs) are the significantly longer c axis [a = 8.5367(4) Å, b = 10.2206(5) Å, c = 16.4268(8) Å at 270 K] compared with the other two, and the presence of intermolecular π–π stacking interactions between uncoordinated and coordinated 2-pyridyl rings with a short centroid to centroid distance of ∼3.6 Å at room temperature with an offset of ∼1.3–1.4 Å. In addition to the latter feature, the crystal structure of **A** is characterized[45] by intermolecular H bonds along the same direction (Fig. S1, ESI†) as the acceptor. These intermolecular interactions boost the formation of a crystal expanded into a specific direction along a certain axis. All these three characteristics were giving us hope for the development of NWs.

In the present study, we have discovered a simple one-pot procedure that leads to the isolation of NWs of **A.** Reaction of a Me_2CO solution of $FeSO_4 \cdot 7H_2O$ and a Me_2CO solution of KSCN (molar ratio 1 : 2), removal of the precipitated K_2SO_4 by filtration and addition of a MeOH solution of abpt (2.0 equiv.), followed by strong stirring, resulted in the rapid formation of a pink crystalline solid. The product was isolated by filtration after 25 min of stirring and washed with cold MeOH and Et_2O. All manipulations were performed in an inert atmosphere (N_2). Typical yields were in the 25–30% range. The crystals were analyzed perfectly for $[Fe(NCS)_2(abpt)_2]$. The procedure is absolutely reproducible. It should be mentioned at this point that
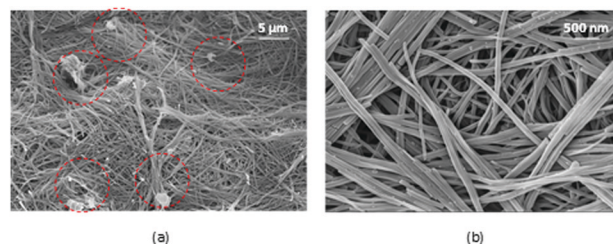
single crystals (i.e., not nanosized material) of **A** had been obtained either from $MeOH/H_2O$[44] or from $MeOH/CH_2Cl_2$;[40] in both cases the crystallization period was long (up to 4 weeks).

Scanning electron microscopy (SEM) images of the isolated material at two different magnifications are shown in Fig. 1. With respect to its morphological characteristics, the material appears fairly homogeneous consisting of highly anisotropic NWs; typical diameters range from ∼40 to ∼160 nm and the associated length is at least a few hundred times larger. Statistics on the measured diameters for 150 NWs resulted in the diameter distribution depicted in Fig. S2 (ESI†); the most typical diameter found is ∼65 nm. Although bundling of a small number of wires is seen in some cases (this indicates the existence of intermolecular interactions along the wires), isolated NWs are also clearly observed. The material contains a very low concentration of white-greyish grains (dashed circles in Fig. 1a); these grains were removed under a stereomicroscope and proved to be polymorph **B** based on the temperature variation of their Raman spectrum (Fig. S3, ESI†).

UV/Vis, ATR/FT-IR and Raman spectra at room temperature (Fig. S4 and S5, ESI†) provide strong evidence that the obtained pink NWs represent polymorph **A**. Upon cooling, the color of the NWs changes to purple, indicative of the SCO transition. Since identification of **A** and **B** is straightforward from their distinctive Raman spectra (Fig. S3, ESI†) and additionally any color discrepancies could be readily observed through the high magnification images of the optical microscope coupled to the micro Raman setup, the temperature dependence of the Raman profile of the NWs can be safely considered as describing the SCO transition of the polymorph **A** NWs.

The raw variable-temperature Raman spectra of a single spot on the NWs (Fig. S6, ESI†) are characterized by the progressive intensity enhancement of some vibrational peaks (additional and/or already existing ones at the room-temperature spectrum) as the temperature decreases. Three spectral regions show clearly this dependence (Fig. 2). In the region below 500 cm^{-1} associated with the Fe^{II}–N vibrational modes, two new bands at 165 cm^{-1} (assigned to the NFeN bending vibration involving the axial Fe^{II}–$N_{isothiocyanato}$ bonds of the LS form) and 464 cm^{-1} (assigned to a stretching vibration of the equatorial Fe^{II}–N bonds in the LS species) appear as the temperature decreases from RT to 76 K and subsequently their intensity progressively increases, being able to be easily distinguished even at 273 K. The full HS → LS transition upon cooling to 80 K is furthermore indicated by the intensity alterations and
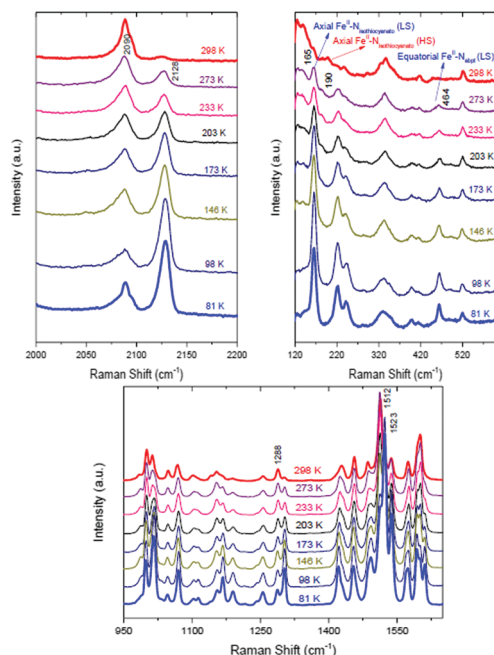
Fig. 2 *In situ* temperature-dependent Raman spectra of the polymorph A of *trans*-[Fe(NCS)$_2$(abpt)$_2$] in the three spectral regions discussed in the text.

shifts of bands attributed to internal vibrations of the coordinated abpt (at ~1300 and ~1510 cm^{-1}) and to the carbon–nitrogen stretching mode of isothiocyanato ligands (in the 2080–2130 cm^{-1} region). The experimental results are in agreement with the DFT calculations on both the HS and LS states (see ESI,† Fig. S7–S9 and Tables S1–S3).

The population of the LS and HS states as a function of temperature may be at least semi-quantitatively extracted by Raman spectroscopy after proper assignment of peaks associated with LS and HS species, respectively, and subsequent calculation of their intensities at various temperatures.[38,39] However, since the intensity of the Raman peaks depends not only on the population of the scattering species and the inelastic scattering cross section of each vibrational mode but also on the temperature, the extraction of species population should be handled with caution. Thus, quantitative results can be obtained using the general formula LS^R = $\frac{I^a}{I^a + kI^b}$ (HS^R + LS^R = 1), where I^a and I^b are the reduced Raman intensities[46] of the a and b vibrational modes that describe LS and HS species, respectively, and K is a proportionality constant introduced in order to compensate for the difference in the Raman cross section between the two vibrational modes. The modes a and b should be in principle chosen so that $I^a \approx 0$ and $I^b \approx 0$ at high and low temperatures, respectively (see ESI,† Fig. S10). A set of peaks that could be used for the extraction of the HS population as a function of temperature in the case of A NWs is the one used for [Fe{N(CN)$_2$}$_2$(abpt)$_2$] NPs,[38] *i.e.* the bands at 165 cm^{-1} (LS) and 190 cm^{-1} (HS), both assigned to a deformation NFeN mode. However, the intensity of a very weak peak at ~190 cm^{-1} in the Raman spectra of A NWs (which could be assigned to the HS species) decreases quickly upon cooling and it is hardly observed at

203 K. Due to the low intensity of this {FeN$_6$} peak in the HS state, the HS → LS transition can not be adequately monitored throughout the 300–80 K range using this pair of peaks.

Two peaks that could be used for the demonstration of the transition are the 165 cm^{-1} peak and the one at 2090 cm^{-1}, whose intensity dependence upon temperature is converse. The results shown in Fig. 3 were obtained after appropriately introducing the reduced representation and after approximating the K value by normalizing the reduced Raman intensities of I^{165} at 80 K and I^{2090} at ambient temperature.[47] In the same figure, HS population data points using different pairs are also given, *i.e.* the 165, 1288 cm^{-1} pair and the 2128, 2090 cm^{-1} one. The respective magnetic susceptibility data[42] for powdered single-crystal samples of A are also included for comparison. The curves obtained from the three different pairs of Raman peaks indicate a gradual SCO transition in the case of NWs that is in contrast to the sharp transition characterizing the polycrystalline sample. The vibrational modes indicative of the LS species are clearly visible even at temperatures 10 K below the room temperature and their intensities increase progressively upon cooling. It is not valid to give a certain value for $T_{1/2}$, because data below 80 K are required. In spite of this, the $T_{1/2}$ value derived from Raman spectroscopy appears to be close to that derived from magnetic data. The phenomenon of *severe* smoothness of the SCO transition temperature profile in 1D nanostructures has previously been reported for NWs of a mononuclear Fe(III) complex with a {Fe^{III}N$_4$O$_2$} coordination sphere.[32] Therefore, in our case the smoothness of the SCO transition observed, when downsizing from micro to nanoscale, is attributed to the fact that at the nanoscale the cooperativity, which stabilizes the spin states, decreases, reinforcing a tendency of their uncertainty. The synergistic morphology effect, due to the NW formations, further intensifies this smoothening. With two examples at hand (polymorph A and the {Fe^{I}N$_4$O$_2$} compound) it appears that the confinement of a SCO system in 1D nanostructures affects the SCO transition in a similar manner. If this behavior is universal for 1D SCO nanostructures or even for other types of NW formation remains an open question.

In summary, the important messages of our work are: (a) a simple one pot route for the synthesis of NWs of molecular materials has been achieved for the first time. More specifically, the use of exclusively wet chemistry appears unprecedented for the
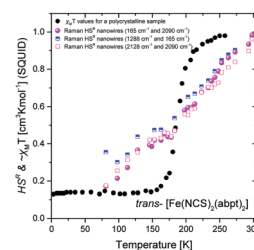

Fig. 3 Temperature dependence of the HS population (in the form of HS^R) extracted from reduced Raman spectra for three different pairs of vibrational bands of *trans*-[Fe(NCS)$_2$(abpt)$_2$] NWs (polymorph A). Magnetic susceptibility data[37] of the same polymorph (powdered single crystals) are also presented for comparison.

preparation of NWs of a SCO system. (b) The SCO transition has been monitored by temperature-dependent micro-Raman spectroscopy which indicated strong deviation from the sharp transition of the polycrystalline samples of **A** at approximately the same $T_{1/2}$ value ($\sim$190 K). The smearing out of the transition is attributed to the morphological characteristics of the sample and it is so strong that a measurable amount of the LS component has been detected at temperatures close to ambient; and (c) the reduced Raman representation was introduced for the first time in SCO systems in order to obtain the temperature-dependent HS population from different sets of vibrational peaks attributed to HS and LS states. Further support of our belief that a remarkably longer unit cell axis appears to favor rapid formation of NWs through entirely wet chemistry (see our selection criteria in the introduction) comes from the preparation and preliminary characterization of a mononuclear Mn(III) SCO complex [monoclinic, Cc, a = 14.9671(4) Å, b = 22.9481(5) Å, c = 14.3590(4) Å at 293 K].[48]

Conflicts of interest

There are no conflicts to declare.

References

1 M. Jacoby, Interview of the 2021 Priestley Medalist A. P. Alivisatos, *Chem. Eng. News*, 2021, **99**, 24–35.
2 Y. Xia, P. Yang, Y. Sun, Y. Wu, B. Mayers, B. Gates, Y. Yin, F. Kim and H. Yan, *Adv. Mater.*, 2003, **15**, 353–389.
3 E. Garnett, L. Mai and P. Yang, *Chem. Rev.*, 2019, **119**, 8955–8957.
4 L. Tsakalakos, J. Balch, J. Fronheiser, B. A. Korevaar, O. Sulima and J. Rand, *Appl. Phys. Lett.*, 2007, **91**, 233117.
5 L.-G. Qiu, Z.-Q. Li, Y. Wu, W. Wang, T. Xu and X. Jiang, *Chem. Commun.*, 2008, 3642–3644.
6 X. Liu, P. Lin, X. Yan, Z. Kang, Y. Zhao, Y. Lei, C. Li, H. Du and Y. Zhang, *Sens. Actuators, B*, 2013, **176**, 22–27.
7 S. Biju, R. O. Freire, Y. K. Eom, R. Scopelliti, J.-C. G. Bünzli and H. K. Kim, *Inorg. Chem.*, 2014, **53**, 8407–8417.
8 N. I. Goktas, P. Wilson, A. Ghukasyan, D. Wagner, S. McNamee and R. R. LaPierre, *Appl. Phys. Rev.*, 2018, **5**, 041305.
9 C. N. R. Rao and A. Govindaraj, *Nanotubes and Nanowires*, The Royal Society of Chemistry, London, U.K., 2nd edn, 2011, ch. 3, pp. 343–353.
10 L. Thomas, M. Hayashi, X. Jiang, R. Moriya, C. Rettner and S. Parkin, *Science*, 2007, **315**, 1553–1556.
11 G. Woltersdorf and C. H. Back, *Phys. Rev. Lett.*, 2007, **99**, 227207.
12 U. Ebels, A. Radulescu, Y. Henry, L. Piraux and K. Ounadjela, *Phys. Rev. Lett.*, 2000, **84**, 983–986.
13 L. Guo, X. Wang, C. Zhong and L. Li, *J. Appl. Phys.*, 2012, **111**, 026104.
14 S. M. Reddy, J. J. Park, S.-M. Na, M. M. Maqableh and A. B. Flatau, *Adv. Funct. Mater.*, 2011, **21**, 4677–4683.
15 P. Gütlich, Y. Garcia and H. A. Goodwin, *Chem. Soc. Rev.*, 2000, **29**, 419–427.
16 P. Gamez, J. S. Costa, M. Quesada and G. Aromí, *Dalton Trans.*, 2009, 7845–7853.
17 M. C. Muñoz and J. A. Real, *Coord. Chem. Rev.*, 2011, **255**, 2068–2093.
18 M. A. Halcrow, *Chem. Soc. Rev.*, 2011, **40**, 4119–4142.
19 R. W. Hogue, S. Singh and S. Brooker, *Chem. Soc. Rev.*, 2018, **47**, 7303–7338.
20 See the various chapters in: M. A. Halcrow, *Spin-Crossover Materials: Properties and Applications*, Wiley, New York, U. S. A., 2013.
21 J.-F. Létard, P. Guionneau and L. Goux-Capes, *Spin Crossover in Transition Metal Compounds III*, Springer, Berlin Heidelberg, 2004, pp. 221–249, DOI: 10.1007/b95429.
22 V. Shalabaeva, K. Ridier, S. Rat, M. D. Manrique-Juarez, L. Salmon, I. Séguy, A. Rotaru, G. Molnár and A. Bousseksou, *Appl. Phys. Lett.*, 2018, **112**, 013301.
23 A. Gee, A. H. Jaafar, B. Brachňaková, J. Massey, C. H. Marrows, I. Šalitroš and N. T. Kemp, *J. Phys. Chem. C*, 2020, **124**, 13393–13399.
24 C.-M. Jureschi, J. Linares, A. Boulmaali, P. R. Dahoo, A. Rotaru and Y. Garcia, *Sensors*, 2016, **16**, 187.
25 K. Boukheddaden, M. H. Ritti, G. Bouchez, M. Sy, M. M. Dîrtu, M. Parlier, J. Linares and Y. Garcia, *J. Phys. Chem. C*, 2018, **122**, 7597–7604.
26 A. Bousseksou, G. Molnár, L. Salmon and W. Nicolazzi, *Chem. Soc. Rev.*, 2011, **40**, 3313–3335.
27 Y.-H. Luo, C. Chen, G.-W. Lu, D.-L. Hong, X.-T. He, C. Wang, J.-Y. Wang and B.-W. Sun, *J. Phys. Chem. Lett.*, 2018, **9**, 7052–7058.
28 L. Salmon and L. Catala, *C. R. Chim.*, 2018, **21**, 1230–1269.
29 S. Usmani, M. Mikolasek, A. Gillet, J. Sanchez Costa, M. Rigoulet, B. Chaudret, A. Bousseksou, B. Lassalle-Kaiser, P. Demont, G. Molnár, L. Salmon, J. Carrey and S. Tricard, *Nanoscale*, 2020, **12**, 8180–8187.
30 O. Trotsenko, A. Tokarev, A. Gruzd, T. Enright and S. Minko, *Nanoscale*, 2015, **7**, 7155–7161.
31 N. Daro, T. Vaudel, L. Afindouli, S. Marre, C. Aymonier and G. Chastanet, *Chem. – Eur. J.*, 2020, **26**, 16286–16290.
32 P. N. Martinho, T. Lemma, B. Gildea, G. Picardi, H. Müller-Bunz, R. J. Förster, T. E. Keyes, G. Redmond and G. G. Morgan, *Angew. Chem., Int. Ed.*, 2012, **51**, 11995–11999.
33 For example, see: A. Bousseksou, J. J. McGarvey, F. Varret, J. A. Real, J.-P. Tuchagues, A. C. Dennis and M. L. Boillot, *Chem. Phys. Lett.*, 2000, **318**, 409–416.
34 For example, see: H. L. C. Feltham, C. Johnson, A. B. S. Elliott, K. C. Gordon, M. Albrecht and S. Brooker, *Inorg. Chem.*, 2015, **54**, 2902–2909.
35 T. Forestier, S. Mornet, N. Daro, T. Nishihara, S.-I. Mouri, K. Tanaka, O. Fouché, E. Freysz and J.-F. Létard, *Chem. Commun.*, 2008, 4327–4329.
36 G. Molnár, S. Cobo, J. A. Real, F. Carcenac, E. Daran, C. Vieu and A. Bousseksou, *Adv. Mater.*, 2007, **19**, 2163–2167.
37 S. Sakaida, K. Otsubo, M. Maesato and H. Kitagawa, *Inorg. Chem.*, 2020, **59**, 16819–16823.
38 Z. G. Lada, K. S. Andrikopoulos, A. Chrissanthopoulos, S. P. Perlepes and G. A. Voyiatzis, *Inorg. Chem.*, 2019, **58**, 5183–5195.
39 Z. G. Lada, K. S. Andrikopoulos, C. D. Polyzou, V. Tangoulis and G. A. Voyiatzis, *J. Raman Spectrosc.*, 2020, **51**, 2171–2181.
40 N. Moliner, M. C. Muñoz, S. Létard, J.-F. Létard, X. Solans, R. Burriel, M. Castro, O. Kahn and J. A. Real, *Inorg. Chim. Acta*, 1999, **291**, 279–288.
41 A. B. Gaspar, M. C. Muñoz, N. Moliner, V. Ksenofontov, G. Levchenko, P. Gütlich and J. A. Real, *Monatsh. Chem.*, 2003, **134**, 285–294.
42 C.-F. Sheu, S.-M. Chen, S.-C. Wang, G.-H. Lee, Y.-H. Liu and Y. Wang, *Chem. Commun.*, 2009, 7512–7514.
43 C.-H. Shih, C.-F. Sheu, K. Kato, K. Sugimoto, J. Kim, Y. Wang and M. Takata, *Dalton Trans.*, 2010, **39**, 9794–9800.
44 H. E. Mason, W. Li, M. A. Carpenter, M. L. Hamilton, J. A. K. Howard and H. A. Sparkes, *New J. Chem.*, 2016, **40**, 2466–2478.
45 Derived from the cif of the compound [CCDC code: 1422236†].
46 G. N. Papatheodorou and S. N. Yannopoulos, in *Molten Salts: From Fundamentals to Applications*, ed. M. Gaume-Escard, Kluwer Academic, Dordrecht, The Netherlands, 2002, pp. 47–106.
47 The K value could be alternatively extracted by assuming that the $T_{1/2}$ value for the polycrystalline and nano-wired systems is the same. The values extracted by the two methodologies were found to be similar.
48 V. B. Jakobsen, E. Trzop, L. C. Gavin, E. Dobbelaar, S. Chikara, X. Ding, K. Esien, H. Müller-Bunz, S. Felton, V. S. Zapf, E. Collet, M. A. Carpenter and G. G. Morgan, *Angew. Chem., Int. Ed.*, 2020, **59**, 13305–13312.